

Model of localized highly frustrated ferromagnetism: The *kagomé* spin ice

A. S. Wills,* R. Ballou, and C. Lacroix

Laboratoire Louis Néel, CNRS, 25 Avenue des Martyrs, Boîte Postal 166, 38042 Grenoble Cedex 9, France

(Received 26 July 2001; revised manuscript received 9 August 2002; published 14 October 2002)

A model of localized highly frustrated ferromagnetism is presented: *kagomé* spin ice. Using analytical and Monte Carlo calculations its massive ground-state entropy is evaluated. Monte Carlo calculations are also used to explore the phases in the presence of further-neighbor interactions and applied fields. The importance of thermal spin fluctuations and their ability to stabilize a variety of magnetic structures is clearly manifested. Remarkably, some of these phases are only partially ordered and present both disordered and ordered sublattices.

DOI: 10.1103/PhysRevB.66.144407

PACS number(s): 75.10.-b, 75.25.+z, 75.40.-s

I. INTRODUCTION

Geometric frustration refers to the inability of a magnetic system to minimize its individual exchange interactions, as a simple consequence of the exchange geometry. For many years it was thought to be limited to antiferromagnets, with much research focusing on the *kagomé* and pyrochlore antiferromagnets,^{1–5} until a phase termed “spin ice” was discovered by Harris and coworkers.^{6–8} In their system, which is based on the pyrochlore lattice, the large number of degenerate ground states that characterize frustrated magnetism is a consequence of particular Ising anisotropies and ferromagnetic nearest-neighbor exchange. Mapping the spin directions onto the disordered hydrogen bonds of Pauling’s cubic ice model, their system was shown to remain disordered even at $T=0$. However, if other terms are present, such as dipolar interactions, a transition to long-range order has been found due to collective zero-energy flips of loops of spins.⁹ Despite the unique properties of pyrochlore spin ice, nothing is known about two-dimensional (2D) spin-ice models or more generally about the properties of frustrated 2D ferromagnetic systems. In contrast, the ice models were widely investigated in two dimensions, especially on a square lattice, a version of which was solved exactly by Lieb.^{10,11} Extensions and generalizations of the model to other lattices soon followed.^{11,12}

In this paper we examine the single-layer *kagomé* ferromagnet with in-plane Ising anisotropies and identify a spin-ice system—*kagomé* spin ice. Using analytic and classical Monte Carlo calculations we demonstrate the massive ground-state degeneracy of this icelike phase, which greatly exceeds that of the pyrochlore spin ice. Furthermore, we show how its degeneracy is raised by additional parameters in the Hamiltonian, namely, second-neighbor interactions or an applied magnetic field, and that these lead to the stabilization of a number of exotic magnetic phases.

II. THE ICE RULES

These local conditions define whether a spin configuration lies within the ground-state manifold. For the pyrochlore system,^{6–8} where the Ising axes point towards the center of the basic tetrahedral motif, the ice rules are that two spins enter and two spins leave each tetrahedron. In the case of the

2D *kagomé* lattice, where the Ising axes now point towards the center of the triangular motif, the ice rules are that either two spins enter and one leaves each triangle, or the converse. Inspection quickly reveals that there are six possible ground-state configurations associated with each triangular motif. These are demonstrated in Fig. 1(a). Extension of the motifs in two dimensions shows that *kagomé* spin ice possesses an extensive degeneracy, the residual entropy of which is calculated in Sec. III.

III. RESIDUAL ENTROPY IN THE MANNER OF PAULING

The residual entropy of cubic ice, and thus of pyrochlore spin ice, has been evaluated by Pauling¹³ as $S_p = (Nk/2)\ln 3/2$. While this value is very close to the exact one evaluated numerically,¹⁴ we note that in fact Pauling’s estimation is that of a Bethe lattice of tetrahedra: starting from an arbitrarily chosen “central” tetrahedron, 6 of the $2^4=16$ possible spin states correspond to spin-ice configurations. As the four neighboring tetrahedra each have one spin fixed due to sharing with the central tetrahedron, they each have only three possible ice states, from a complete manifold

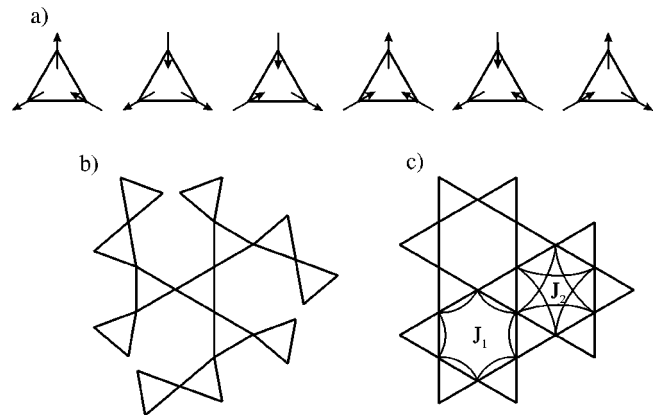


FIG. 1. (a) The six degenerate spin configurations for a single triangle of the *kagomé* spin-ice model with the Ising axes pointing to the center of each triangle. The Bethe lattice (b) and the *kagomé* lattice (c) of vertex sharing triangles. The nearest-neighbor and second-neighbor interactions, J_1 and J_2 respectively, of the *kagomé* lattice are defined separately in (c).

of $2^3=8$ states. The same argument can then be used for all tetrahedra as one moves out through the Bethe lattice. Thus, among the 2^N possible states (N being the total number of sites), only a fraction $(\frac{3}{8})^{N_T}$ (N_T being the number of tetrahedra, i.e., $N_T=N/2$) satisfy the ice rule on all tetrahedra, which leads to an entropy: $S_p = k \ln[2^N \times (\frac{3}{8})^{N_T}] = (Nk/2) \ln 3/2$. In the pyrochlore lattice, closed loops have to be taken into account: for one tetrahedron with two spins fixed by the neighboring tetrahedra, the number of acceptable ice states is either one or two (depending on the configuration of the two fixed spins), among four possible configurations for the two remaining spins; this leads again to an average reduction factor of $\frac{3}{8}$, while if three spins are fixed this factor is larger: $\frac{1}{2}$. Thus for a lattice of tetrahedra, the number of ice states should be slightly larger than the Pauling value S_p , as has been found numerically $S_n = 1.01 S_p$.¹⁴ As previously demonstrated for more general ice models,¹² Pauling's estimate is a lower bound on the exact value of the entropy.

The estimation of the residual entropy for a Bethe lattice of triangles [Fig. 1(b)] can be made following the same principles: for each triangle with one fixed spin, the number of ice states is equal to three, while the number of possible states is $2^2=4$. Thus, if N_T is now the number of triangles, the total number of ice states is $2^N \times (\frac{3}{4})^{N_T}$, (with $N_T = 2N/3$), leading to an entropy $S_b = Nk/3 \ln 9/2$. If we again consider the effect of the closed loops present in the *kagomé* lattice [Fig. 1(c)], we find that if two spins are fixed for a given triangle, the number of acceptable states for the third spin is either one or two, among two possible states. Assuming that the states with two spins fixed are equiprobable, an average factor $\frac{3}{4}$ is again obtained. Although this procedure ignores any correlations beyond the first neighbors, this simplified argument suggests that closed loops should not be expected to change that much the entropy in the *kagomé* lattice and the exact value should be very close to S_b . Our numerical estimations show clearly that this is the case. In fact this spin ice *kagomé* system can be mapped exactly on the Ising *kagomé* antiferromagnet, in a similar way as the pyrochlore system.^{15,16} Consequently, the value that we found for the entropy is the same that was found for the disordered ground state of the antiferromagnetic Ising *kagomé* system.^{17,18}

IV. MONTE CARLO CALCULATIONS

Our classical¹⁹ simulations were made on a single *kagomé* plane of 50×50 unit cells, each containing three spins of modulus $S = 1$, i.e., 7500 spins in total. The nearest- and the second-neighbor exchange integrals, J_1 and J_2 , were used to couple the spins according to the pathways shown in Fig. 1(d). A Kirkpatrick²⁰ cooling scheme was used with each step in temperature involving a reduction from T_1 to T_2 according to the equation $T_2 = 0.9T_1$. At each temperature 5000 cycles site^{-1} were used for equilibration and 5000 cycles site^{-1} for the calculation of the thermodynamic properties. The starting temperature for all the simulations was $T = 10|J_1|S^2$. The spin maps presented are representative of

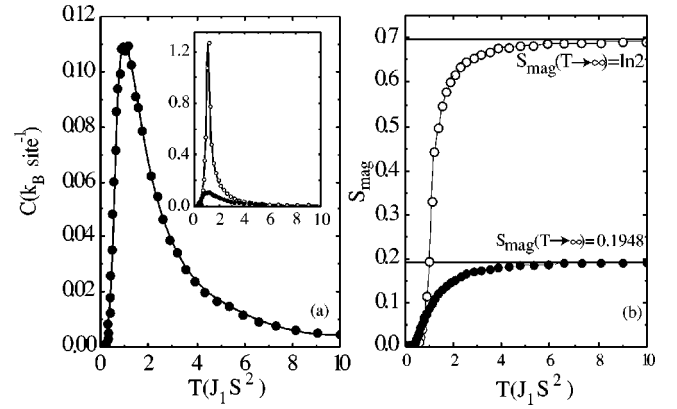


FIG. 2. (a) The specific heat and the (b) magnetic entropy of *kagomé* spin ice (●) and the related antiferromagnetic system (○) as a function of temperature. Due to their differing scales, the comparison between the specific heat of the two systems is shown as an inset. The limiting values of their magnetic entropies, S_{mag} , as $T \rightarrow \infty$ are shown.

the average over the Monte Carlo cycles performed at each temperature that are within the specified range.

The Hamiltonian can be defined as

$$H = - \sum_{i,j < i} J_{ij} \vec{S}_i \cdot \vec{S}_j + H_A - (g \mu_B) \vec{H} \cdot \sum_i \vec{S}_i, \quad (1)$$

where the anisotropy term H_A reads $\sum_i \kappa_i (\vec{S}_i \cdot \hat{x}_i)^2$, $\kappa_i < 0$ is the single-ion anisotropy constant that forces the local spin \vec{S}_i to align along the local axis \hat{x}_i and \vec{H} is the applied field. In order to create Ising spins with the different local orientations shown in Fig. 1, the transverse spin fluctuations were completely frozen out, which corresponds to setting $\kappa_i = -\infty$.

V. THERMODYNAMIC PROPERTIES AND SPIN CORRELATIONS OF KAGOMÉ SPIN ICE

The specific heat of *kagomé* spin ice shows a broad maximum at $T/J_1 S^2 = 1$. Above this temperature, in the range $1 < T/J_1 S^2 < 2$, the slow approach of the magnetic entropy to its saturation level reveals the presence of significant short-ranged order correlations. The residual entropy of the spin-ice state is clearly discernible in the magnetic entropy (Fig. 2) as the shortfall in the high-temperature limit with respect to the $\ln 2$ expected for Ising spins as $T \rightarrow \infty$. If the limiting value of the integrated entropy is taken as 0.1948(35), we find that the residual entropy of the spin-ice phase is $S_{mag}(T=0) = S_{mag}(T=\infty) - \int_0^\infty (C/T) dT = \ln 2 - 0.1948 = 0.4982(35)$, a value that is in good agreement with the residual entropy of $S_b = \frac{1}{3} \ln 9/2 = 0.5014$ calculated for the Bethe lattice.

As a contrast, the entropy of the antiferromagnetic system ($J_1 < 0$) with the same Ising anisotropies as the spin-ice phase is also shown in Fig. 2. While a maximum in the specific heat is also seen at $T_c = |J_1| S^2$ [Fig. 2(a)], the magnetic entropy differs sharply from the *kagomé* spin ice, in that it involves a recovery of the complete $S = \ln 2$ value

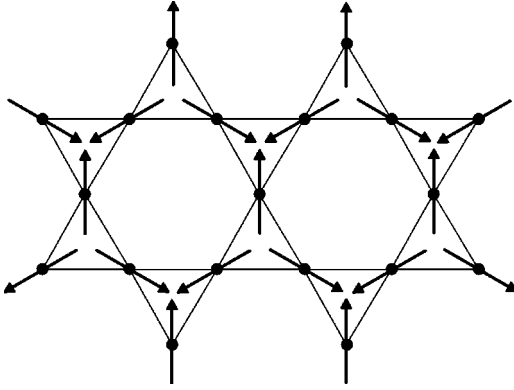


FIG. 3. The $q=0$ ground state of the *kagomé* antiferromagnet.

expected for the formation of long-range order. The long-range order that results is the so-called $q=0$ spin structure familiar in *kagomé* antiferromagnets² and is shown in Fig. 3.

Equal time correlations $\langle \vec{S}_i \cdot \vec{S}_j \rangle$ between distant spins \vec{S}_i and \vec{S}_j , averaged over the Monte Carlo cycles at equilibrium, were computed at different temperatures. Figure 4 shows the thermal variations obtained for the first and second spin neighbors. An increase in absolute values is observed as the temperature is decreased, down to $T \sim 0.5|J_1|S^2$ at which the correlations saturate.

The correlations at zero temperature in the spin-ice phase are evaluated analytically for the Bethe lattice of triangles for all neighbors as $\langle \vec{S}_i \cdot \vec{S}_j \rangle_b = (\frac{-1}{3})^m \cos \theta_{ij}$, where m is the number of bonds that form the path joining the spins \vec{S}_i and \vec{S}_j , and θ_{ij} is the angle difference $\theta_j - \theta_i$ between the orientations of the local anisotropy axes \hat{x}_i and \hat{x}_j for these spins. Numerical values for different neighbors $\vec{S}_\beta, \vec{S}_\gamma, \dots$ of a given spin \vec{S}_α as specified in Fig. 5 are reported in Table I, and are compared to the correlations for corresponding neighbors in the *kagomé* lattice, which were computed at the lowest temperature ($T \sim 0.0004J_1S^2$) of the Monte Carlo simulations. Agreement is remarkable, except for the $\vec{S}_\alpha - \vec{S}_\delta$ spin pairs. This is to be expected as in the *kagomé*

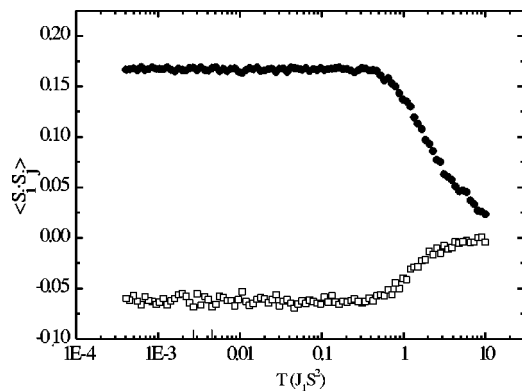


FIG. 4. A semilog plot of the first (●) and second neighbor (□) spin-spin correlations in *kagomé* spin ice as a function of temperature.

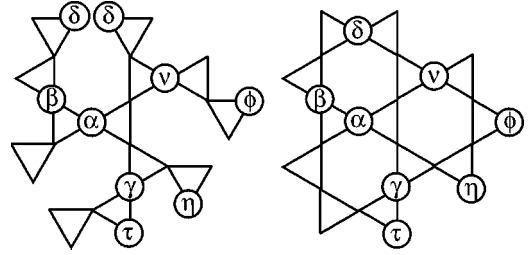


FIG. 5. Neighborhood of a given spin \vec{S}_α in the Bethe and the *kagomé* lattice of triangles.

lattice these neighbors belong to the same hexagon and are thus connected by two paths with exactly the same number of bonds, which leads to correlations that are larger by a factor of ~ 2 . In a similar way the other distant spins in the *kagomé* lattice, such as the second neighbors, are also not connected by only one path; however, as these other paths have a larger number of bonds and the concomitant corrections decay as a power law in the number of bonds, they give rise to only minor adjustments.

VI. ANTIFERROMAGNETIC SECOND-NEIGHBOR INTERACTIONS

These were examined with the values of $J_2/J_1 = -0.4, -0.2$ and -0.1 . In all cases three features are seen in the specific heat (Fig. 6). The first at $T \sim J_1S^2$ involves the formation of short-ranged spin-ice-type correlations. Below this temperature, at $T \sim 1.5|J_2|S^2$, the additional antiferromagnetic exchange stabilizes a partially ordered structure that is made up of clockwise and counterclockwise hexagons of spins [Fig. 7(a)]. The mean magnitude of the moments on the sublattice that separate these hexagons is zero. The reason for some of the sites failing to order is made clear from examination of the lowest maximum at $T \sim |J_2|S^2$: this involves the formation of an ordered magnetic structure that has a unit cell that is three times larger along each of the axes than the paramagnetic cell [Fig. 7(b)]. The complexity of this structure is evidenced from the two types of hexagons: the clockwise hexagons (and the time-reversed counterclockwise) are separated by those that have three pairs of parallel spins. As the latter involve adjacent spins with antiferromagnetic 120° orientations, this ground state configuration is

TABLE I. Spin-spin correlations in the Bethe and *kagomé* lattice of triangles between a given spin \vec{S}_α and its neighbors as specified in Fig. 5 (n th: order of neighborhood in the *kagomé* lattice).

ij	m	θ_{ij}	$\langle \vec{S}_i \cdot \vec{S}_j \rangle_b$	n^{th}	$\langle \vec{S}_i \cdot \vec{S}_j \rangle$
$\alpha \beta$	1	$\pm 2\pi/3$	$1/6 = 0.166\ 67$	1st	0.166
$\alpha \gamma$	2	$\pm 2\pi/3$	$-1/18 = -0.055\ 56$	2nd	-0.059
$\alpha \nu$	2	0	$1/9 = 0.111\ 11$	3rd	0.101
$\alpha \delta$	3	0	$-1/27 = -0.037\ 04$	3rd	-0.072
$\alpha \tau$	3	$\pm 2\pi/3$	$1/54 = 0.017\ 54$	4th	0.012
$\alpha \eta$	3	$\pm 2\pi/3$	$1/54 = 0.017\ 54$	5th	0.017
$\alpha \phi$	4	0	$1/81 = 0.012\ 34$	6th	0.007

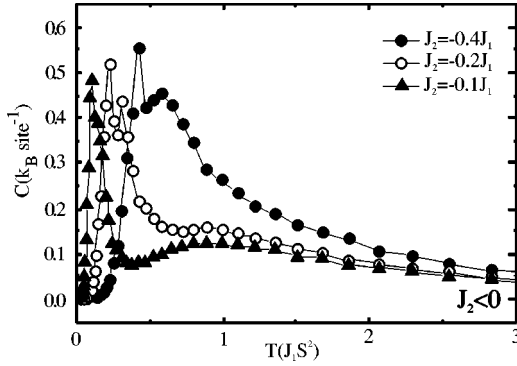


FIG. 6. Specific heat for the Ising *kagomé* ferromagnet with second-neighbor interactions: $J_2 < 0$.

frustrated. Reexamination of the intermediate phase ($|J_2|S^2 < T < 1.5|J_2|S^2$) shows that the fluctuations have selectively annulled the mean moment on sites that would otherwise frustrate the lattice.

As J_2/J_1 is increased, the intermediate phase becomes stable over a wider temperature range; when $J_2/J_1 = -0.4$ this phase occurs at temperatures from $0.4J_1S^2$ to $0.6J_1S^2$.

VII. FERROMAGNETIC SECOND-NEIGHBOR INTERACTIONS

As the lattice of second neighbors is also a *kagomé* lattice, ferromagnetic J_2 still result in a highly frustrated spin system and if the moments related by J_1 and J_2 are of uniform magnitude 1/3 of the moments lie on sites of zero mean field (Fig. 8). It is not surprising, therefore, that extensive fluctuations are still present at the lowest temperatures for all the values of $J_2 > 0$ studied ($J_2/J_1 = 0.4, 0.2$, and 0.1), in sharp contrast with the ground state when $J_2 < 0$. If these second-neighbor interactions present a minor contribution to the Hamiltonian, e.g., $J_2/J_1 = 0.1$, short-ranged icelike correlations still form and these give rise to a broad feature in the specific heat at $T \sim J_1S^2$ (Fig. 9). However, in contrast with the $J_2 < 0$ phases, only one maximum is seen at lower temperature, $T \sim J_2S^2$. Remarkably, this is not associated with a phase transition and no long-range order is seen down to the lowest temperature: only a tendency is observed that involves the condensation of a partially ordered phase with the propagation vector $\mathbf{k} = (00)$ and a nonzero ferromagnetic component (Fig. 8). These correlations are strongest when J_2 is weakest. As J_2 increases, this tendency dwindles out and

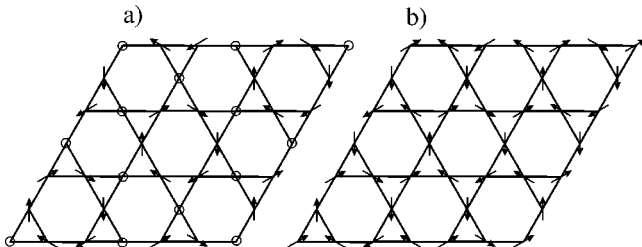


FIG. 7. Averaged Monte Carlo spin maps of the structures for $J_2 < 0$ when (a) $|J_2|S^2 < T < 1.5|J_2|S^2$ (b) $T \leq |J_2|S^2$. Open circles represent disordered spins.

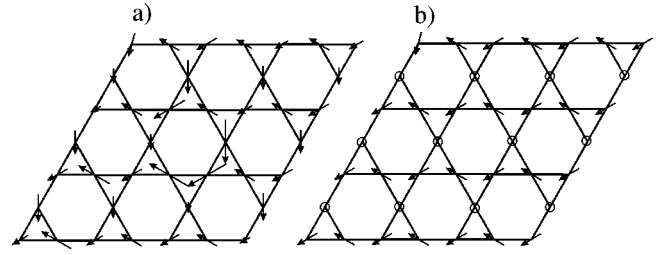


FIG. 8. While no long-range order occurs, tendencies towards order with particular structures are seen. These spin maps are presented for $J_2 \geq 0$ when (a) $T \leq J_2S^2$ (b) $T \leq J_2S^2$. Open circles represent disordered spins.

the two maxima in the specific heat merge. What remains are strongly fluctuating phases with correlations that are less and less reminiscent of the partially ordered phase.²¹

VIII. EFFECTS OF MAGNETIC FIELD

The effects of an externally applied magnetic field on the spin-ice phase were studied with fields of up to $0.269J_1S$ applied along the characteristic directions of the *kagomé* lattice, i.e., \mathbf{a} and \mathbf{a}^* (Fig. 10). These calculations were made at a temperature of $0.025J_1S^2$ after the system had been cooled in zero applied field.

With the field parallel to the \mathbf{a} direction, a continuous increase in an ordered component is observed. Notably, it involves only 2/3 of the sites [Fig. 10(a)]. This demonstrates another point of similarity between the 2D *kagomé* spin-ice system and that of the closely related 3D pyrochlore lattice: the spin components induced by a field along some of the crystallographic directions are not capable of choosing a unique ground state and significant degeneracy is retained. A common result is the formation of only partially ordered spin configurations.

With the field parallel to the \mathbf{a}^* direction a continuous increase of order with the $\mathbf{k} = (00)$ structure [Fig. 10(b)] is again found. Trivially, we find that the ordering is preferential for the sites with their local anisotropy parallel to the field direction. The ordered component of all the sites saturates in a field of $0.054J_1S$.

An inspection of the high-field ordered structures suggests that even an infinitesimal field applied along either of the

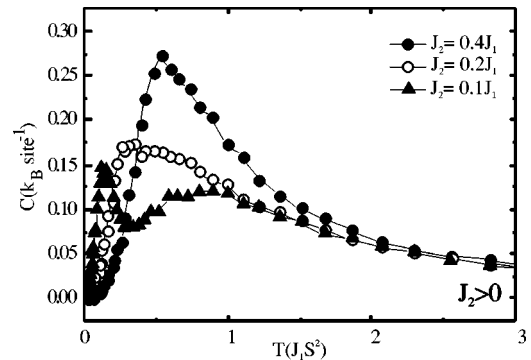


FIG. 9. Specific heat for the Ising *kagomé* ferromagnet with second-neighbor interactions: $J_2 > 0$.

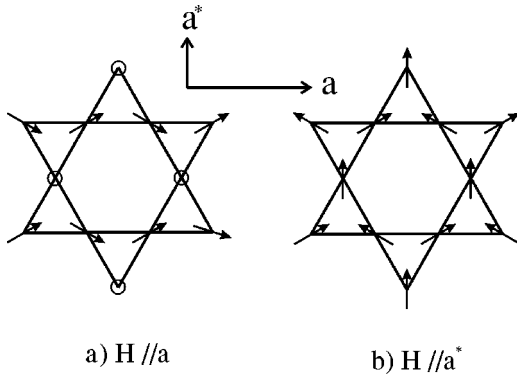


FIG. 10. The high-field spin configurations when the applied field is along the \mathbf{a} and \mathbf{a}^* directions. Open circles represent disordered spins, i.e., those that have equal probability of being in either direction.

characteristic directions would induce an ordered component. It is therefore a surprise that the initial dependence of the reduced magnetization on the field is not sharper. Our simulations show that this weaker dependence is a result of thermal fluctuations, rather than being a consequence of the finite lattice size. This is demonstrated by the collapse of the reduced magnetization as a function of the Zeeman energy divided by the thermal energy, onto the same curve at all temperatures studied (see Figs. 11 and 12).

IX. DISCUSSION

The thermodynamic properties of *kagomé* spin ice, and those of phases in the presence of second-neighbor interactions and applied fields, manifest clearly the richness of frustrated physics once thought to be the domain only of antiferromagnets. In particular, the importance of spin fluctuations is central and their presence leads to the stabilization of a variety of magnetic structures with both disordered and ordered sublattices. While such partially ordered phases have

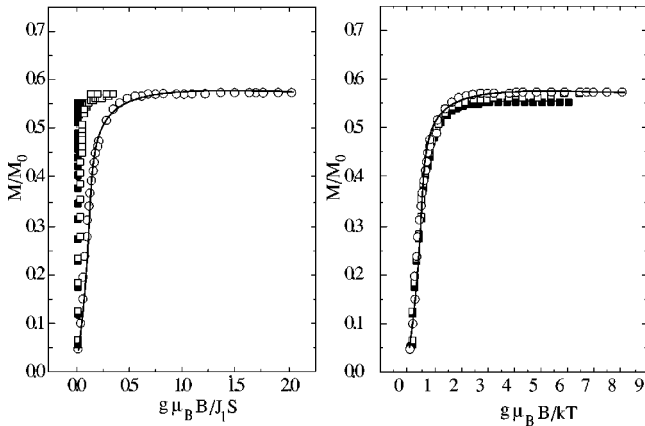


FIG. 11. The reduced magnetization per site as a function of applied field along the \mathbf{a} direction (a) in units of the molecular field $J_1 S$ and (b) after rescaling the applied field with temperature, i.e., plotting M/M_0 vs $\mu_B B g/kT$, a universal curve is obtained. The temperatures of the field sweeps were (\circ) 0.254, (\square) 0.051, (\bullet) 0.010, and (\blacksquare) $0.002J_1 S^2$. The line provides guide to the eye.

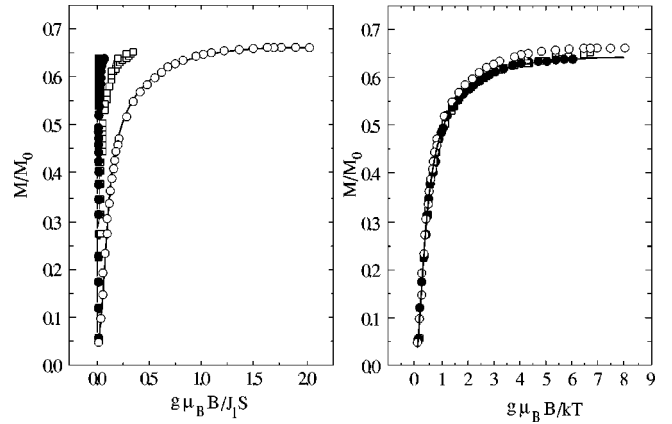


FIG. 12. The reduced magnetization per site as a function of applied field along the \mathbf{a}^* direction (a) in units of the molecular field $J_1 S$ and (b) after rescaling the applied field with temperature, i.e., plotting M/M_0 vs $\mu_B B g/kT$, a universal curve is obtained. The temperatures of the field sweeps were (\circ) 0.254, (\square) 0.051, (\bullet) 0.010, and (\blacksquare) $0.002J_1 S^2$. The line provides guide to the eye.

already been found to be stable in frustrated lattices when the local moments are close to an instability²² or in systems with contrived further-neighbor exchange,²³ here they are stable with well-defined magnetic moments and are a simple consequence of the strong frustration associated with uniaxial anisotropy. In real systems²⁴ additional terms such as quantum fluctuations and dipolar interactions will be present in the Hamiltonian. While further work is required to determine how these will alter the spin-ice phase and the partially ordered phases presented here, these effects have already been shown to be strongly influential on their low-temperature physics. A review of how Ising models are influenced by the introduction of quantum dynamics that arises from the inclusion of an XY exchange component is presented in Ref. 26. An interesting limit for their inclusion is the XY antiferromagnetic on a pyrochlore lattice model presented by Champion *et al.*,²⁷ in which a spin-wave analysis indicated that zero-point quantum fluctuations stabilize the formation of an ordered moment from the a highly degenerate continuous manifold.

The observation that the ordered Néel state proposed²⁸ for the vanadium jarosite $(\text{H}_3\text{O})\text{V}_3(\text{SO}_4)_2(\text{OH})_6$ is a highly symmetric member of the spin-ice manifold suggests that spin-ice-like correlations will be present above, but close to, its ordering temperature. The system is clearly not a true realization of *kagomé* spin ice as the presence of a transition to Néel order requires that either additional terms in the exchange Hamiltonian that we have not considered here have raised the degeneracy of the icelike manifold, or that the single-ion anisotropies it possesses are of a magnitude for which quantum fluctuations are important. Unfortunately, the single-ion terms in the jarosite are difficult to estimate because the relative contributions of axial (DS_z^2) and rhombic [$E(S_x^2 - S_y^2)$] terms determined from magnetic susceptibility data²⁹ taken from $\text{KGa}_{2.96}\text{V}_{0.04}(\text{SO}_4)_2(\text{OH})_6$ are ambiguous, as other pair (D, E) parameters may fit them equally well. However, it is still reasonable that the short-range correla-

tions present above the ordering temperature will be characteristic of the most important terms in the Hamiltonian, and thus of the spin-ice phase.

In conclusion, we have presented a model of localized highly frustrated ferromagnetism: *kagomé* spin ice. If residual entropy is used as a measure of frustration, our analytical and numerical calculations demonstrate that *kagomé*

spin ice is more highly frustrated than the 3D counterpart, pyrochlore spin ice. It is therefore the most highly geometrically frustrated “ferromagnetic” ground state yet to be studied. Furthermore, second-neighbor interactions within the *kagomé* plane are shown to have the salient effect of stabilizing structures that feature both ordered and disordered sublattices.

*Present address: Dept. of Chemistry, Christopher Ingold Laboratories, University College London, 20 Gordon Street, London, WC1H 0AJ, UK.

¹J. Villain, *Z. Phys.* **33**, 31 (1979).

²A.B. Harris, C. Kallin, and A.J. Berlinsky, *Phys. Rev. B* **45**, 2899 (1992).

³A.P. Ramirez, *Annu. Rev. Mater. Sci.* **24**, 453 (1994).

⁴J.E. Greedan, *J. Mater. Chem.* **11**, 37 (2001).

⁵*Proceedings of the Highly Frustrated Magnetism 2000 Conference, Waterloo, Canada, 2000*, [Can. J. Phys. **79**, 11-12 (2001)].

⁶M.J. Harris, S.T. Bramwell, D.F. McMorrow, T. Zeiske, and K.W. Godfrey, *Phys. Rev. Lett.* **79**, 2554 (1997).

⁷M.J. Harris, S.T. Bramwell, P.C.W. Holdsworth, and J.D.M. Champion, *Phys. Rev. Lett.* **81**, 4496 (1998).

⁸S.T. Bramwell and M.J. Harris, *J. Phys.: Condens. Matter* **10**, L215 (1998).

⁹B.C. den Hertog, R.G. Melko, and M.J.P. Gingras, cond-mat/0009225 (unpublished).

¹⁰E.H. Lieb, *Phys. Rev.* **162**, 162 (1967); *Phys. Rev. Lett.* **18**, 1046 (1967); **19**, 108 (1967).

¹¹R. J. Baxter, *Exactly Solved Models in Statistical Mechanics* (Academic, London, 1982).

¹²E. H. Lieb and F. Y. Wu, in *Phase Transitions and Critical Phenomena*, edited by C. Domb and M. H. Green (Academic, London, 1972), Vol. 1, pp. 332–410.

¹³L. Pauling, *The Nature of the Chemical Bond* (Cornell University Press, Ithaca, NY, 1960), pp. 301–304.

¹⁴J.F. Nagle, *J. Math. Phys.* **7**, 1484 (1966).

¹⁵R. Liebmann, *Statistical Mechanics of Periodic Frustrated Ising Systems* (Springer-Verlag, New York, 1986), pp. 117–122.

¹⁶M.J. Harris, S.T. Bramwell, D.F. McMorrow, T. Zeiske, and K.W. Godfrey, *Phys. Rev. Lett.* **79**, 2554 (1997).

¹⁷R. Liebmann, *Statistical Mechanics of Periodic Frustrated Ising Systems* (Springer-Verlag, New York, 1986), pp. 77–81.

¹⁸D.A. Huse and A.D. Rutenberg, *Phys. Rev. B* **45**, 7536 (1992).

¹⁹We note that quantum fluctuations cannot play a role in the physics of spin ice systems at low temperature since these states require large Ising anisotropies that will freeze them out.

²⁰S. Kirkpatrick, C.D. Gelatt, and M.P. Vecchi, *Science* **220**, 671 (1983).

²¹The possibility of such fluctuating phases is discussed in R. Ballou, *J. Alloys Compd.* **275-277**, 510 (1998).

²²R. Ballou, C. Lacroix, and M.D. Nunez-Regueiro, *Phys. Rev. Lett.* **66**, 1910 (1991); M.D. Nunez-Regueiro and C. Lacroix, *Phys. Rev. B* **50**, 16 063 (1994); C. Lacroix, B. Canals, and M.D. Nunez-Regueiro, *Phys. Rev. Lett.* **77**, 5126 (1996); R. Ballou, *J. Alloys Compd.* **275-277**, 510 (1998).

²³O. Nagai, T. Horiguchi, and S. Miyashita, in *Magnetic Systems with Competing Interactions* edited by H. T. Diep (World Scientific, Singapore, 1994), pp. 202–237.

²⁴Since the submission of this manuscript a *kagomé* spin ice phase has been stabilized in $\text{Dy}_2\text{Ti}_2\text{O}_7$ by the application of a magnetic field along the $\langle 111 \rangle$ direction (Ref. 25).

²⁵K. Matsuhira, Z. Hiroi, T. Tayama, S. Takagi, and T. Sakakibara, *J. Phys.: Condens. Matter* **14**, L559 (2002); K. Matsuhira, Z. Hiroi, T. Tayama, S. Takagi, and T. Sakakibara, cond-mat/0207543 (unpublished).

²⁶R. Moessner and S.L. Sondhi, *Phys. Rev. B* **63**, 224401 (2001).

²⁷J.D.M. Champion, M.J. Harris, P.C.W. Holdsworth, A.S. Wills, G. Balakrishnan, S.T. Bramwell, E. Cizmar, T. Fennell, J.S. Gardner, J. Lago, D.F. McMorrow, M. Orendac, A. Orendacova, D.McK. Paul, R.I. Smith, M.T.F. Telling, and A. Wildes, cond-mat/0112007 (unpublished).

²⁸A.S. Wills, *Phys. Rev. B* **63**, 064430 (2001).

²⁹D. Papoutsakis, D. Grohol, and D.G. Nocera, *J. Am. Chem. Soc.* **124**, 2647 (2002).